

# 1 Identification and quantification of Lyme pathogen strains by deep 2 sequencing of outer surface protein C (*ospC*) amplicons

---

3 Lia Di<sup>1</sup>, Zhenmao Wan<sup>2</sup>, Saymon Akther<sup>2</sup>, Chunxiao Ying<sup>1</sup>, Amanda Larracuente<sup>2</sup>, Li Li<sup>2</sup>, Chong  
4 Di<sup>1</sup>, Roy Nunez<sup>1</sup>, D. Moses Cucura<sup>3</sup>, Noel L. Goddard<sup>1,2</sup>, Konstantino Krampus<sup>1,2,4</sup>, and Wei-Gang  
5 Qiu<sup>1,2,4,#</sup>

6 <sup>1</sup>Department of Biological Sciences, Hunter College of the City University of New York, 695 Park  
7 Avenue, New York 10065, USA

8 <sup>2</sup>Graduate Center of the City University of New York, 365 Fifth Avenue, New York 10016, USA

9 <sup>3</sup>Division of Vector Control, Suffolk County Department of Public Works, Yaphank, New York  
10 11980, USA

11 <sup>4</sup>Department of Physiology and Biophysics & Institute for Computational Biomedicine, Weil  
12 Cornell Medical College, New York, New York 10021, USA

13 <sup>#</sup>Correspondence: Weigang Qiu, [weigang@genectr.hunter.cuny.edu](mailto:weigang@genectr.hunter.cuny.edu)

14 Authors' emails & project roles:

- 15 • Lia Di [dilie66@gmail.com](mailto:dilie66@gmail.com): Methodology, Investigation, Data Curation, Software, Visualization
- 16 • Zhenmao Wan [wanzhenmao@gmail.com](mailto:wanzhenmao@gmail.com): Methodology, Investigation, Writing (original draft)
- 17 • Saymon Akther [saymon.akther@gmail.com](mailto:saymon.akther@gmail.com): Methodology, Investigation, Resources
- 18 • Chunxiao Ying [chunxiao.ying@gmail.com](mailto:chunxiao.ying@gmail.com): Investigation
- 19 • Amanda Larracuente [aslarracuente@gmail.com](mailto:aslarracuente@gmail.com): Investigation
- 20 • Li Li [gift4lily@gmail.com](mailto:gift4lily@gmail.com): Resources, Investigation
- 21 • Chong Di [chongdi0505@gmail.com](mailto:chongdi0505@gmail.com): Resources, Visualization
- 22 • Roy Nunez [roynunez273@gmail.com](mailto:roynunez273@gmail.com): Resources
- 23 • D. Moses Cucura [Moses.Cucura@suffolkcountyny.gov](mailto:Moses.Cucura@suffolkcountyny.gov): Resources
- 24 • Noel Goddard [goddard.noel@gmail.com](mailto:goddard.noel@gmail.com): Supervision, Funding acquisition
- 25 • Konstantino Krampus [agbiotec@gmail.com](mailto:agbiotec@gmail.com): Methodology, Funding acquisition, Writing (review &  
26 editing)
- 27 • Weigang Qiu [weigang@genectr.hunter.cuny.edu](mailto:weigang@genectr.hunter.cuny.edu): Conceptualization, Funding acquisition,  
28 Supervision, Writing (original draft)

29 Short Title: Genotyping Lyme pathogens from ticks

30

## 31 **Abstract**

32 Mixed infection of a single tick or host by Lyme disease spirochetes is common and a  
33 unique challenge for diagnosis, treatment, and surveillance of Lyme disease. Here we describe a  
34 novel protocol for differentiating Lyme strains based on deep sequencing of the hypervariable  
35 outer-surface protein C locus (*ospC*). Improving upon the traditional DNA-DNA hybridization  
36 method, the next-generation sequencing-based protocol is high-throughput, quantitative, and able  
37 to detect new pathogen strains. We applied the method to over one hundred infected *Ixodes*  
38 *scapularis* ticks collected from New York State, USA in 2015 and 2016. Analysis of strain  
39 distributions within individual ticks suggests an overabundance of multiple infections by five or  
40 more strains, inhibitory interactions among co-infecting strains, and presence of a new strain  
41 closely related to *Borrelia bissettiae*. A supporting bioinformatics pipeline has been developed.  
42 With the newly designed pair of universal *ospC* primers targeting intergenic sequences conserved  
43 among all known Lyme pathogens, the protocol could be used for culture-free identification and  
44 quantification of Lyme pathogens in wildlife and clinical specimens across the globe.

45

46 **Key Words:** Lyme disease, *Borrelia*, *Borrelia*, *Ixodes scapularis*, outer surface protein  
47 C, next-generation sequencing, frequency-dependent selection

## 48 **Introduction**

49 Lyme disease occurs throughout the Northern Hemisphere and is the most prevalent vector-  
50 borne diseases in the United States (Hengge et al., 2003; Margos et al., 2011; Schwartz et al.,  
51 2017). The causative agents of Lyme disease are obligate bacterial parasites of vertebrates  
52 transmitted predominantly by hard-bodied *Ixodes* ticks. Lyme pathogens and related strains,  
53 formerly known as the *Borrelia burgdorferi* *sensu lato* species group, have been recently (and  
54 controversially) classified as a new spirochetal genus *Borrelia* (Adeolu and Gupta, 2014;  
55 Margos et al., 2017). In the US, while *B. burgdorferi* causes the majority of the Lyme disease  
56 cases, more than a half dozen additional *Borrelia* species have been recognized including *B.*  
57 *americana*, *B. andersonii*, *B. bissettiae*, *B. californiensis*, *B. carolinensis*, *B. kurtenbachii*, and *B.*  
58 *mayonii* (Dolan et al., 2016; Marconi et al., 1995; Margos et al., 2016, 2013; Bobbi S. Pritt et al.,  
59 2016; Rudenko et al., 2011, 2009). *Borrelia* species vary not only in genomic sequences but

60 also in geographic distribution, host preferences, human pathogenicity, and disease manifestations  
61 (Barbour et al., 2009; Casjens et al., 2018; Kurtenbach et al., 2006; Margos et al., 2011; Mongodin  
62 et al., 2013; Bobbi S Pritt et al., 2016). In addition, the *Ixodes* ticks in the US and elsewhere are  
63 frequently co-infected with *Borrelia miyamotoi*, a member of the re-defined *Borrelia* genus now  
64 consisting exclusively of strains grouped with agents of relapsing fever (Barbour et al., 2009;  
65 Wagemakers et al., 2015).

66 A hallmark of Lyme disease endemics is the coexistence of multiple spirochete species and  
67 strains within local populations and oftentimes within a single vector, host or patient (Brisson and  
68 Dykhuizen, 2004; Durand et al., 2017; Guttman et al., 1996; Qiu, 2008; Seinost et al., 1999; Walter  
69 et al., 2016; Wang et al., 1999; Wormser et al., 2008). High genetic diversity within local pathogen  
70 populations is to a large extent driven and maintained by frequency-dependent selection under  
71 which rare strains gain selective advantage over common ones in establishing super-infection in a  
72 host (Bhatia et al., 2018; Durand et al., 2017; Haven et al., 2011; States et al., 2014). In addition,  
73 local con-specific strains may have diverged in host specificity and other phenotypes including  
74 human virulence and invasiveness (Brisson and Dykhuizen, 2004; Hanincova et al., 2013; Seinost  
75 et al., 1999; Wormser et al., 2008). Against this backdrop of the vast geographic, genetic, and  
76 phenotypic variations of Lyme disease pathogens across the globe and within endemic regions, it  
77 is essential to develop accurate, sensitive, and scalable technologies for identifying species and  
78 strains of Lyme pathogens in order to understand, monitor, and control the range expansion of  
79 Lyme disease (Kilpatrick et al., 2017; Kurtenbach et al., 2006; Qiu and Martin, 2014).

80 Early molecular technologies for identifying Lyme pathogen strains relied on amplifying  
81 and detecting genetic variations at single variable locus including the outer-surface protein A locus  
82 (*ospA*), outer surface protein C locus (*ospC*), and the intergenic spacer regions of ribosomal RNA  
83 genes (*rrs-rrlA* and *rrfA-rrlB*) (Guttman et al., 1996; Wang et al., 2014, 1999). Availability of the  
84 first Lyme pathogen genome facilitated development of more sensitive multilocus sequence typing  
85 (MLST) technologies targeting genetic variations at a set of single-copy housekeeping genes  
86 (Fraser et al., 1997; Hanincova et al., 2013; Qiu, 2008). For direct identification of Lyme strains  
87 in tick and host specimen without first culturing and isolating the organisms, a reverse-line blotting  
88 (RLB) technology has been developed based on DNA-DNA hybridization (Brisson and  
89 Dykhuizen, 2004; Durand et al., 2015; Morán Cadenas et al., 2007; Qiu et al., 2002). The RLB  
90 technology, while sensitive and able to detect mixed infection in tick and hosts, is difficult to scale

91 up or to standardize and does not yield quantitative measures of strain diversity. A further  
92 limitation of the RLB technology is that it depends on oligonucleotide probes of known *ospC*  
93 major-group alleles and is not able to detect strains with novel *ospC* alleles.

94 Next-generation sequencing (NGS) technologies circumvent the limitations of traditional  
95 methods in scalability, standardization, and ability for *de novo* strain detection while offering high  
96 sensitivity and high throughput quantification (Lefterova et al., 2015). Using the hybridization  
97 capture technology to first enrich pathogen genomes in ticks and subsequently obtaining genome-  
98 wide short-read sequences using the Illumina NGS platform, >70% of field-collected nymphal  
99 ticks from Northeast and Midwest US are found to be infected with multiple *B. burgdorferi* strains  
100 due to mixed inoculum (Walter et al., 2016). In an NGS-based study of European Lyme pathogen  
101 populations, a combination of quantitative PCR and high-throughput sequencing on the 454  
102 pyrosequencing platform targeting the *ospC* locus and revealed a similarly high rate (77.1%) of  
103 mixed infection of nymphal ticks by *B. afzelii* and *B. garinii* (Durand et al., 2017).

104 Here we report an improved NGS technology for identifying Lyme pathogen strains  
105 through deep sequencing of *ospC* sequences amplified from individual ticks. We applied the  
106 technology to over 100 pathogen-infected *Ixodes scapularis* ticks collected from New York State  
107 during a period of two years. Our results suggest a new putative *Borrelia* species, competitive  
108 interactions among co-infecting strains, and genetic homogeneity within an endemic region.

## 109 Materials & Methods

### 110 Tick collection and DNA extraction

111 Adult and nymphal blacklegged ticks (*Ixodes scapularis*) were collected in 2015 and 2016  
112 during their host-seeking seasons from four locations in endemic areas of Lyme disease  
113 surrounding New York City (Figure 1). Ticks are stored at -80°C before dissection. Each tick is  
114 immersed in 5% solution of Chelex 100 resin (Sigma-Aldrich, St. Louis, MO, USA) containing  
115 20mg/ml Proteinase K in milliQ water (EMD Millipore, Billerica, MA, USA) with a total volume  
116 of 30µl for nymphs, 100µl for males, and 200µl for females. Ticks are dissected into four or more  
117 pieces using sterilized scalpel or disposable pipette tips. The dissected mixture is incubated at 56°C  
118 overnight and heated to 100°C for 10 minutes afterwards in a dry bath, and then briefly centrifuged

119 to separate the tick debris and Chelex resin from the supernatant. The supernatant containing the  
120 extracted DNA is transferred to a fresh tube and stored at 4°C (or frozen at -20°C for long term  
121 storage).

122 **Single-round PCR amplification of full-length *ospC***

123 An improved protocol for amplifying *ospC* sequences from tick DNA extracts has been  
124 developed. First, this protocol is simpler with a single instead of two rounds of polymerase-chain  
125 reaction (Brisson and Dykhuizen, 2004; Qiu et al., 2002). Second, using a newly designed  
126 oligonucleotide primer pair targeting flanking intergenic sequences conserved across *Borrelia*  
127 species, we are able to amplify full-length (~718 bp) *ospC* sequences from all strains. Third, the  
128 new primers are able to amplify a *vsp* locus in the *B. miyamotoii* genome, enabling co-detection of  
129 *Borrelia* species and *Borrelia miyamotoii*, two major groups of Lyme pathogens in Northeast  
130 US (Barbour et al., 2009). The new primer sequences are 5'-  
131 AATAAAAAGGAGGCACAAATTAAATG-3' ("Oc-Fwd", targeting the intergenic spacer  
132 between BB\_B18 and BB\_B19) and 5'-ATATTGACTTATTTCAGTTAC-3' ("Oc-Rev",  
133 targeting the intergenic spacer between BB\_B19 and BB\_B22). Alignments of primer regions for  
134 Lyme pathogens are provided as Supplemental Material S1.

135 Each 20μl reaction mixture contains 200 μM of each dNTP, 1U Roche FastStart Taq DNA  
136 polymerase (Roche Diagnostics, Mannheim, Germany), 2μl of 10x Roche FastStart Buffer (Roche  
137 Diagnostics, California, USA), 0.4μM of each primer and 1μl DNA extract. The reaction mixture  
138 is heated at 95°C for 4 minutes, then amplified for 36 cycles at 95°C for 30 seconds, 58°C for 30  
139 seconds, and 72°C for 60 seconds, and finally incubated at 72°C for 5 minutes. The PCR products  
140 are electrophoresed on a 1% agarose gel, stained with ethidium bromide, and imaged under a UV  
141 light. Agencourt AMPure XP PCR Purification Kit (Beckman Coulter, Brea, CA, USA) is used to  
142 remove excess primers, dNTPs, and other reagents. Amplicon quantity is measured on the Qubit 4  
143 Fluorometer (Thermo Fisher Scientific, Waltham, MA, USA) using the companying Qubit  
144 dsDNA HS Assay Kit.

145 **NGS library preparation and short-read sequencing**

146 We followed the Nextera XT DNA Library Prep (Illumina, CA, USA, catalog no. FC-131-  
147 1024) protocol to prepare the amplicon libraries for sequencing. First, we dilute the PCR products  
148 to 0.2ng/μl after DNA quantification using a DNA 1000 kit on a 2100 BioAnalyzer (Agilent, Santa

149 Clara, CA, USA). Samples are fragmented by incubation of 5 $\mu$ l DNA sample in 55°C for 5 minutes  
150 in a solution containing 10 $\mu$ l Tagment DNA Buffer and 5 $\mu$ l Amplicon Tagment Mix.  
151 Tagmentation reaction is terminated by adding 5 $\mu$ l Neutralize Tagment Buffer. Tagmented  
152 samples are amplified and barcoded (with Set A and Set B) using PCR in a solution containing 5 $\mu$ l  
153 of each barcoded primers and the Nextera PCR Mater Mix. The thermal cycling parameters are  
154 incubation at 72°C for 3 minutes, 95°C for 30 seconds, 12 cycles of 95°C for 10 seconds, 55°C for  
155 30 seconds, and 72°C for 30 seconds, and a final incubation at 72°C for 5 minutes. The indexed  
156 amplicon libraries are cleaned using AMPure XP PCR Purification Kit and concentrations  
157 quantified using the High-Sensitivity DNA 1000 Kit on a 2100 BioAnalyzer. Amplicon libraries  
158 are diluted to the same concentration and then combined to a total concentration of 2 nM to 4 nM  
159 with a volume of 5 $\mu$ l or more.

160 In preparation for loading on the MiSeq sequencer, the pooled library is denatured by  
161 mixing 5 $\mu$ l of 0.2N NaOH with 5 $\mu$ l of sample and incubating at room temperature for 5 minutes  
162 and then adding 990 $\mu$ l pre-chilled Hybridization Buffer, resulting in a total of 1 ml (10pM  
163 concentration) of denatured pooled amplicon library (Illumina Denature and Dilute Libraries  
164 Guide pub. no. 15039740). Furthermore, 5% PhiX Sequencing Control (Illumina, CA, USA,  
165 catalog no. FC-110-3001) is added to the samples pool before loading to the MiSeq. The  
166 sequencing kit used is the MiSeq Reagent Kit v3 for 150 cycles (Illumina, CA, USA, catalog no.  
167 MS-102-3001), for paired reads of 75 bases each. Following sequencing, a total of 4.24 gigabases  
168 of sequence are generated by the instrument, corresponding to 57,463,220 reads, with  
169 approximately 90% of the reads (52,311,968) passing the filter build-in the MiSeq for quality  
170 control. Finally, the samples are automatically de-multiplexed to individual FASTQ files following  
171 completion of the sequencing run by the MiSeq Reporter Software based on the Nextera XT  
172 barcodes corresponding to each sample (the barcodes are also trimmed by the software from each  
173 read).

#### 174 **Amplicon cloning & Sanger sequencing**

175 New alleles are identified when the majority of reads are not aligned to reference  
176 sequences. For such samples, we performed *de novo* assembly of short reads to obtain candidate  
177 allele sequences (see below). The novel alleles are subsequently validated by cloning and Sanger  
178 sequencing. Cloning of PCR products is performed using the TOPO TA Cloning Kit for

179 Sequencing (Thermo Fisher Scientific, Waltham, MA, USA) following manufacturer's protocol.  
180 Five bacterial colonies containing plasmids with PCR amplicon as inserts are selected for further  
181 growth in selective liquid media. Plasmid DNA is extracted and purified using the PureLink Quick  
182 Plasmid Miniprep Kits (Thermo Fisher Scientific, Waltham, MA, USA). Nucleotide sequences of  
183 cloned PCR amplicons are obtained using the Sanger method through commercial sequencing services  
184 including Genewiz (South Plainfield, NJ, USA) and Macrogen (Rockville, MD, USA).

### 185 **Bioinformatics methods for allele identification and quantification**

186 Alleles present in tick samples are identified and quantified by aligning the paired-end  
187 short reads to a set of reference sequences. These reference sequences consist of full-length *ospC*  
188 sequences and are obtained from published genome sequences, from Sanger sequencing of cloned  
189 or uncloned amplicons (see above), or from *de novo* assembly of short reads (see below) (the 20  
190 reference sequences are listed in Supplemental Material S2).

191 The short reads are indexed and aligned to the reference sequences using software packages  
192 bwa (Li and Durbin, 2009) and samtools (Li et al., 2009). Coverage of reads at each site of each  
193 reference sequence is obtained by using bedtools (Quinlan and Hall, 2010) and visualized using  
194 ggplot2 in the R statistical computing environment (R Core Team, 2013; Wickham, 2009).  
195 Presence of new alleles is noted when a large number of reads are unmapped. For these samples,  
196 we cloned the PCR amplicons and sequenced the clones using Sanger sequencing (see above). A  
197 number of known alleles do not have full-length *ospC* sequences from sequenced genomes or from  
198 GenBank. For these alleles, we performed *de novo* assembly of reads to obtain the 5'- and 3'-end  
199 sequences using the assembler metaSPAdes (Nurk et al., 2017).

200 To test the accuracy and sensitivity of our bioinformatics pipelines, we generated simulated  
201 short reads with known allele identities and known proportions of allele mixture using wgsim, a  
202 part of the software samtools package (Li et al., 2009). Key steps and commands for allele  
203 identification, coverage calculation, *de novo* assembly, and simulated reads are provided as  
204 Supplemental Material S3.

### 205 **Statistical analysis of genetic diversity**

206 We estimate the relative amount of spirochete load in individual infected ticks by the  
207 weight (in ng) of PCR amplicons. Diversity of *ospC* alleles in individual infected ticks is first

208 measured with multiplicity, i.e., the number of unique alleles present in a sample. Allelic diversity  
209 is further measured with the Shannon diversity index  $\alpha = 1 - \frac{-\sum p_i \log(p_i)}{\log(n)}$ , where  $p_i$  is the  
210 frequency of allele  $i$  and  $n$  is the number of distinct alleles in an infected tick (allowing  $\alpha=0$  for  
211  $n=1$ ). This Shannon diversity index, also known as the Shannon Equitability Index, is a normalized  
212 measure of biodiversity ranging from 0 (infected with a single strain) to 1 (all strains being equally  
213 frequent) (Vidakovic, 2011). Allele frequencies in an infected tick are obtained as  $p_i =$   
214  $C_i / \sum_{j=1}^n C_j$ , where  $C_i$  is the coverage of allele  $i$  averaged over all nucleotide positions.

215 Genetic differentiation between two populations (A and B) is measured with the  $F_{st}$   
216 statistics:  $F_{st} = \frac{H_T - [n_A H_S(A) + n_B H_S(B)]}{(n_A + n_B) H_T}$  (Nei, 1973), where  $H_S(A)$ ,  $H_S(B)$ , and  $H_T$  are heterozygosity  
217 of sample A, sample B, and the total sample, respectively, and  $n_A$  and  $n_B$  are the sample sizes.  
218 Statistical significance of an  $F_{st}$  value is estimated by a randomization procedure by which the two  
219 population samples are combined and randomly divided into two pseudo-samples with the same  
220 sample sizes. An  $F_{st}$  value is calculated between the two pseudo-samples. The procedure is  
221 repeated for 999 times and a  $p$ -value is obtain as the proportion of permuted  $F_{st}$  values that is  
222 greater than or equal to the observed value. Genetic differentiation is further tested using  $F$ -  
223 statistics implemented in the *hierfstat* package on the R statistical computing environment  
224 (Goudet, 2005).

## 225 Data availability

226 New sequences have been deposited in GenBank with consecutive accessions MH071430  
227 through MH071436. Experimental data are stored in a custom relational database. An interactive  
228 website has been developed using the D3js (<http://d3js.org>) JavaScript library to visualize allele  
229 composition and read depth for the 119 tick samples and is publicly available at  
230 <http://diverge.hunter.cuny.edu/~weigang/ospC-sequencing/>. Data sets and R scripts are publicly  
231 available at Github <https://github.com/weigangq/ocseq>.

## 232 Results

### 233 Tick infection rates, co-infections, specificity, and sensitivity

234 Approximately 25% of nymphal ticks and 50% of adult ticks are infected with *Borrelia*

235 species or *Borrelia miyamotoi*. For example, the nymphal infection rate for *Borrelia burgdorferi*  
236 is 27.9% (with a 95% confidence interval of 15.3 – 43.7%) in Sample #7 and the adult infection  
237 rate for *Borrelia burgdorferi* is 42.1% (32.9 – 51.7%) for Sample #9 (Figure 1). The infection  
238 rate for *Borrelia miyamotoi* in adult ticks is 6.1% (7 out of 114 ticks; 2.5 – 12.2% confidence  
239 interval) for Sample #9. Four ticks in Sample #9 are infected with both *Borrelia burgdorferi*  
240 and *Borrelia miyamotoi* (co-infection rate 3.5%, 0.96-8.74%). Rates from other samples are  
241 underestimates due to lack of success in tick storage, processing, DNA amplification, and NGS  
242 sequencing during protocol development. These rates are consistent with results from other studies  
243 conducted in the same region and appear to be stable through recent decades (Qiu et al., 2002;  
244 States et al., 2014).

245 The number of sequencing averages ~108,000 reads per tick sample. The coverage (i.e.,  
246 read depth) of an allele depends on the total number of tick samples in a pooled library and the  
247 number of alleles present in a tick. Alleles are identified if the reads cover all nucleotide positions  
248 of a reference allele and the total read percentage is at least 1% of the most abundant alleles. The  
249 total sample of 119 successfully sequenced ticks are divided into four sub-population samples  
250 according to geographic origin and life stage, with allele counts of pathogens in each of the four  
251 populations listed in Table 1.

252 Specificity of allele identification is tested by generating simulated reads from a single  
253 reference sequence and aligning the simulated reads to all reference sequences. This simulation-  
254 based test shows that the bioinformatics protocol for allele identification is highly specific, with  
255 only a small fraction of ambiguously aligned reads at the first ~200 conserved positions for some  
256 *ospC* alleles (Supplemental Material S4).

257 Sensitivity of allele quantification is tested by generating a known proportion of simulated  
258 reads from two reference sequences. For example, a 10:1 mixed sample of short reads generated  
259 based on sequences of alleles “J” and “C” is quantified using the bioinformatics protocol, resulting  
260 in a ~13:1 quantification (Figure 2A).

## 261 **New strain, spirochete load, and multiplicity**

262 The NGS protocol is able to not only detect the presence of multiple strains but also  
263 quantify their relative frequency in individual ticks infected by multiple strains (Figure 2B). One  
264 allele (labeled as “C14\_N150”) does not have known high-identity homologs in GenBank, with

265 the top BLASTp hit as the *B. bissetiae* strain 25015 *ospC* with 75% identity in protein sequence  
266 (ACC45540) (Tilly et al., 1997). This allele likely represents an un-identified *Borrelia* species  
267 (Figure 2C). This allele was cloned, sequenced with Sanger method, and assigned a GenBank  
268 accession (MH071431). The full-length “F” allele was similarly cloned, sequenced with Sanger  
269 method, and assigned a GenBank accession (MH071432). The full-length “O” allele (MH071435)  
270 was sequenced with Sanger method directly from the singly-infected tick #N045 without cloning  
271 of the PCR amplicon. Sequences of full-length alleles “B3”, “N”, and “T” (MH071430,  
272 MH071433, and MH071436) were obtained by *de novo* assembly of short reads using metaSPAdes  
273 (Nurk et al., 2017). Our protocol is able to detect infection by *Borrelia miyamotoi*, as shown by  
274 the presence of one of its *vsp* (variable surface protein gene, locus name AXH25\_04790)  
275 amplicons in samples (Figure 2D). The *vsp* allele was cloned, sequenced with Sanger method, and  
276 assigned a GenBank accession (MH071435).

277 Assuming that the spirochete load is correlated with total weight of PCR amplicons, we  
278 found that female adult ticks carry a significantly higher spirochete load than male adult ticks  
279 ( $p=0.022$  by *t*-test), which in turn carry a higher infection load than nymphal ticks ( $p=8.1e-3$ )  
280 (Figure 3A). There is no significant difference in the average number of strains infecting a single  
281 tick ( $p>0.5$  by Mann-Whitney test), although the median values are two strains per infected adult  
282 tick and one strain per nymphal tick (Figure 3B). Similarly, there are no significant differences in  
283 strain diversity measured by the Shannon diversity index between male, female, and nymphal ticks  
284 ( $p>0.5$  by Mann-Whitney test; Figure 3C).

## 285 **Aggregated infection & negative strain interactions**

286 A previous study of multi-strain infection by *B. afzelii* in Europe found that strains tend to  
287 be aggregated in infected ticks, suggesting that infection of ticks and hosts is more successfully  
288 established by multiple spirochete strains than by a single strain alone (Andersson et al., 2013).  
289 Our data support their conclusion. In Sample #9, for example, we detected a total of 159 *ospC*  
290 alleles in 55 infected ticks out of a total of 114 processed adult ticks. Assuming a Poisson model  
291 of independent infection of individual strains with an average successful infection rate  
292  $\lambda=159/114=1.395$  strains per tick, we expect on average 28.2 uninfected ticks and 39.4 ticks  
293 infected by a single strain (the observed and expected counts are plotted in Figure 3D). In fact, 59  
294 ticks are uninfected in this sample, more than twice the expected count. Meanwhile, 22 ticks are

295 infected by a single strain, approximately half of the expected number. It appears that ticks tend to  
296 be either free of infection or infected by multiple spirochete strains, supporting the aggregated  
297 infection hypothesis (Andersson et al., 2013).

298 In infected ticks, previous studies conclude either a negative or a lack of interactions among  
299 co-infecting strains (Andersson et al., 2013; Durand et al., 2017; Walter et al., 2016). Our analysis  
300 supports presence of negative or inhibitory interactions among co-infecting strains. First, multiple  
301 strains tend to be unevenly distributed in their spirochete loads with some strains dominating others  
302 (e.g., Figure 2B). This is more generally shown with the Shannon diversity index, which is on  
303 average approximately half of the maximum attainable diversity (when all strains are equally  
304 abundant) in ticks with mixed infections (Supplemental Figure S5). There is, however, no evidence  
305 that any particular strains are consistently more dominant than other (Supplemental Figure S5).  
306 Second, when strains are independent from each other or facilitating each other's growth, one  
307 expects ticks infected with multiple strains to have a higher spirochete load than ticks infected with  
308 a single strain. Conversely, if strains inhibit each other within a host or vector, one expects the  
309 total spirochete load to be either lower in ticks infected by multiple than by single strains or at  
310 similar levels. We plot the total pathogen load with respect to multiplicity or the Shannon diversity  
311 index in individual ticks (Figure 4). For the most part, the regression lines are not significantly  
312 different from a slope of zero except that the spirochete load in nymphs decreases significantly  
313 with increasing number of strains. The overall flat trend supports negative rather than facilitating  
314 interactions or a lack of any interactions between co-infecting strains (Durand et al., 2017; Walter  
315 et al., 2016).

### 316 **Similar strain distributions among regions and life stages**

317 Spirochete populations infecting adult and nymph ticks are similar in strain composition  
318 ( $F_{ST}=4.7\text{e-}3$  and  $p=0.089$  by resampling,  $p=0.369$  by  $F$ -test) (Figures 5A & 5C). Genetic  
319 differentiation between the Upper State and Long Island populations is more pronounced but  
320 nonetheless lacks statistical significance ( $F_{ST}=5.3\text{e-}3$  and  $p=0.052$  by resampling,  $p=0.245$  by  $F$ -  
321 test). The groups F and J strains appear to be more common on Long Island than Upper State  
322 while the group L strain shows the opposite pattern of distribution (Figures 5B & D).

## 323 Discussion

324 In this report, we describe a new experimental and bioinformatics protocol for detecting  
325 and quantifying Lyme disease pathogen strains infecting individual ticks based on next-generation  
326 sequencing technology. Improving upon the previous Reverse-Line Blotting technology, the  
327 protocol allows *de novo* detection of previously unknown pathogen strains. Indeed, one of the ticks  
328 carries a putative new *Borrelia* species with a novel *ospC* allele (“C14”, MH071431). The  
329 protocol is highly sensitive and specific, enabling quantification of genetic diversity within single  
330 ticks and rigorously testing ecological hypotheses such as strain interactions (Figures 4) and  
331 genetic differentiation (Figure 5).

332 High-throughput sequencing has previously been used for quantification of Lyme strains  
333 in ticks based on either genome capture or *ospC* amplicons (Durand et al., 2017; Walter et al.,  
334 2016). Our technology is novel for an improved PCR protocol by using a set of universal PCR  
335 primers able to amplify full-length *ospC* in all *Borrelia* species as well as the *vsp* locus in  
336 *Borrelia miyamotoi*. Further, the PCR protocol is simplified from two rounds to a single round of  
337 thermal cycling. Due to these critical improvements in PCR protocol, our method could be readily  
338 used for detection and quantification of a broad range of Lyme disease (and possibly relapsing  
339 fever) pathogens in clinical and wildlife specimens across their species ranges worldwide. In  
340 addition, our technology is novel in using the Illumina short-read sequencing platform, in its  
341 supporting bioinformatics pipelines, and in its application to *Ixodes* ticks in North America.

342 Our strain identification method is based on the assumption of a strict one-to-one  
343 correspondence (i.e., complete genetic linkage) between *ospC* alleles and *B. burgdorferi* strains.  
344 The *ospC* locus is the most polymorphic single-copy locus in the *Borrelia* genome (Mongodin  
345 et al., 2013). The linkage between the *ospC* locus and the whole genome is indeed nearly complete  
346 for *Borrelia* populations in Northeast United States (Casjens et al., 2017; Mongodin et al., 2013).  
347 In fact, diversification of strains in local *Borrelia* populations is likely driven by frequency-  
348 dependent selection targeting the *ospC* locus (Haven et al., 2011; Qiu and Martin, 2014). However,  
349 linkage between *ospC* and other genomic loci is weaker in Midwestern and Southern US  
350 populations due to recombination and plasmid exchange (Hanincova et al., 2013; Mechai et al.,  
351 2015). Cross-species and cross-strain exchange of *ospC* alleles is also common in European  
352 populations. For example, whole genome sequencing showed that the European *B. burgdorferi*

353 strain BOL26 obtained its *ospC* and its flanking genes from a con-specific strain through horizontal  
354 gene transfer (Qiu and Martin, 2014). For population samples elsewhere, therefore, it might be  
355 necessary to add a 2<sup>nd</sup> locus for strain identification (Barbour and Cook, 2018). One complementary  
356 genetic marker could be the rRNA spacer (*rrs-rrlA*), which is a single-copy and highly variable  
357 locus (Wang et al., 2014). Experimental methods for high-throughput sequencing of the *rrs-rrlA*  
358 locus however are yet to be developed.

359 While we are able to estimate relative spirochete loads in individual ticks based on  
360 quantification of *ospC* amplicons (Figure 2A), we have not attempted to directly quantify the  
361 number of spirochetes in infected ticks using methods such as quantitative PCR (Durand et al.,  
362 2017). In the future, we plan to quantify spirochete loads in individual ticks by running our  
363 experimental and bioinformatics procedures with known quantities of genomic DNA and  
364 generating a standard calibration curve.

365 Nonetheless, using relative estimates of spirochete loads in individual ticks, we are able to  
366 validate a number of hypotheses on multi-strain infections. First, the lack of differences in strain  
367 diversity between the questing adult ticks, which have taken two blood meals, and the questing  
368 nymphal ticks, which have taken one blood meal (Figure 3), supports the conclusion that strain  
369 diversity in individual ticks is for the most part due to mixed inoculum in infected hosts (Walter  
370 et al., 2016). Second, ticks are more likely to be infected by five or more strains than expected by  
371 chance (Figure 4D), supporting the aggregated infection hypothesis (Andersson et al., 2013).  
372 Rather than strains actively facilitating each other in establishing infections, however, strain  
373 aggregation in ticks may be a reflection of reservoir hosts being either free of spirochetes (in the  
374 case of resistant and healthy hosts) or infected by multiple strains (in the case of susceptible and  
375 weakened hosts). Regardless, it appears that once a host is infected by a strain, it becomes  
376 susceptible for super-infection by additional, immunologically distinct strains (Bhatia et al., 2018).  
377 Third, we found an uneven distribution of strains in infected ticks as well as a flat or decreasing  
378 spirochete load with increasing strain diversity (Figure 5), supporting inhibitory interactions  
379 among co-infecting strains driven by competitive growth in reservoir hosts (Durand et al., 2017;  
380 Walter et al., 2016). Fourth, we found weak genetic differentiation between populations from the  
381 two New York City suburbs (Figure 5B), suggesting either a recent common origin, or similar  
382 reservoir hosts, or both. Fifth, we observed co-circulation of *B. miyamotoii* and other *Borrelia*  
383 species in the same area. The lower prevalence as well as lower genetic diversity at *ospC* or *vsp*

384 loci of these low-prevalence spirochetes relative to those of *B. burgdorferi* suggests that *ospC*  
385 hypervariability may be a key adaptation underlining the ecological success of *B. burgdorferi* in  
386 this region.

387 To summarize, we have established a next-generation sequencing-based, taxonomically  
388 broad procedure that has the potential to become a standard protocol for detecting and quantifying  
389 Lyme disease pathogens across the globe. The increased sensitivity of high-throughput sequencing  
390 technologies employed here and elsewhere highlights the prevalence of multiple infections in  
391 wildlife samples and a pressing need for broad spectrum vaccines for control and prevention of  
392 Lyme disease (Earnhart et al., 2007; Livey et al., 2011).

## 393 Acknowledgements

394 We thank Ms Li Zhai and Dr Edward Skolnik of New York University School of Medicine  
395 for facilitating cloning experiments and Mr Brian Sulkow for participation of fieldwork. This work  
396 was supported by Public Health Service grants AI107955 (to WGQ) from the National Institute of  
397 Allergy and Infectious Diseases (NIAID) and the grant MD007599 (to Hunter College) from the  
398 National Institute on Minority Health and Health Disparities (NIMHD) of the National Institutes  
399 of Health (NIH) of the United States of America. The content of this manuscript is solely the  
400 responsibility of the authors and do not necessarily represent the official views of NIAID, NIMHD,  
401 or NIH.

## 402 References

403 Adeolu, M., Gupta, R.S., 2014. A phylogenomic and molecular marker based proposal for the division of  
404 the genus *Borrelia* into two genera: the emended genus *Borrelia* containing only the members  
405 of the relapsing fever *Borrelia*, and the genus *Borrelia* gen. nov. containing the members of  
406 the Lyme disease *Borrelia* (*Borrelia burgdorferi* sensu lato complex). *Antonie Van Leeuwenhoek*  
407 105, 1049–1072. <https://doi.org/10.1007/s10482-014-0164-x>

408 Andersson, M., Scherman, K., Råberg, L., 2013. Multiple-strain infections of *Borrelia afzelii*: a role for  
409 within-host interactions in the maintenance of antigenic diversity? *Am. Nat.* 181, 545–554.  
410 <https://doi.org/10.1086/669905>

411 Barbour, A.G., Bunikis, J., Travinsky, B., Hoen, A.G., Diuk-Wasser, M.A., Fish, D., Tsao, J.I., 2009. Niche  
412 partitioning of *Borrelia burgdorferi* and *Borrelia miyamotoi* in the same tick vector and  
413 mammalian reservoir species. *Am. J. Trop. Med. Hyg.* 81, 1120–1131.  
414 <https://doi.org/10.4269/ajtmh.2009.09-0208>

415 Barbour, A.G., Cook, V.J., 2018. Genotyping Strains of Lyme Disease Agents Directly From Ticks, Blood,

416 or Tissue, in: *Borrelia Burgdorferi*, Methods in Molecular Biology. Humana Press, New York, NY,  
417 pp. 1–11. [https://doi.org/10.1007/978-1-4939-7383-5\\_1](https://doi.org/10.1007/978-1-4939-7383-5_1)

418 Bhatia, B., Hillman, C., Carracoi, V., Cheff, B.N., Tilly, K., Rosa, P.A., 2018. Infection history of the  
419 blood-meal host dictates pathogenic potential of the Lyme disease spirochete within the  
420 feeding tick vector. *PLOS Pathog.* 14, e1006959. <https://doi.org/10.1371/journal.ppat.1006959>

421 Brisson, D., Dykhuizen, D.E., 2004. *ospC* Diversity in *Borrelia burgdorferi* Different Hosts Are Different  
422 Niches. *Genetics* 168, 713–722. <https://doi.org/10.1534/genetics.104.028738>

423 Casjens, S.R., Di, L., Akther, S., Mongodin, E.F., Luft, B.J., Schutzer, S.E., Fraser, C.M., Qiu, W.-G.,  
424 2018. Primordial origin and diversification of plasmids in Lyme disease agent bacteria. *BMC*  
425 *Genomics* 19, 218. <https://doi.org/10.1186/s12864-018-4597-x>

426 Casjens, S.R., Gilcrease, E.B., Vujsadinovic, M., Mongodin, E.F., Luft, B.J., Schutzer, S.E., Fraser, C.M.,  
427 Qiu, W.-G., 2017. Plasmid diversity and phylogenetic consistency in the Lyme disease agent  
428 *Borrelia burgdorferi*. *BMC Genomics* 18, 165. <https://doi.org/10.1186/s12864-017-3553-5>

429 Dolan, M.C., Hojgaard, A., Hoxmeier, J.C., Repleglo, A.J., Respicio-Kingry, L.B., Sexton, C., Williams,  
430 M.A., Pritt, B.S., Schriefer, M.E., Eisen, L., 2016. Vector competence of the blacklegged tick,  
431 *Ixodes scapularis*, for the recently recognized Lyme borreliosis spirochete *Candidatus Borrelia*  
432 *mayonii*. *Ticks Tick-Borne Dis.* <https://doi.org/10.1016/j.ttbdis.2016.02.012>

433 Durand, J., Herrmann, C., Genné, D., Sarr, A., Gern, L., Voordouw, M.J., 2017. Multistrain Infections  
434 with Lyme Borreliosis Pathogens in the Tick Vector. *Appl. Environ. Microbiol.* 83, e02552-16.  
435 <https://doi.org/10.1128/AEM.02552-16>

436 Durand, J., Jacquet, M., Paillard, L., Rais, O., Gern, L., Voordouw, M.J., 2015. Cross-Immunity and  
437 Community Structure of a Multiple-Strain Pathogen in the Tick Vector. *Appl. Environ.*  
438 *Microbiol.* 81, 7740–7752. <https://doi.org/10.1128/AEM.02296-15>

439 Earnhart, C.G., Buckles, E.L., Marconi, R.T., 2007. Development of an *OspC*-based tetravalent,  
440 recombinant, chimeric vaccinogen that elicits bactericidal antibody against diverse Lyme  
441 disease spirochete strains. *Vaccine* 25, 466–480. <https://doi.org/10.1016/j.vaccine.2006.07.052>

442 Fraser, C.M., Casjens, S., Huang, W.M., Sutton, G.G., Clayton, R., Lathigra, R., White, O., Ketchum,  
443 K.A., Dodson, R., Hickey, E.K., Gwinn, M., Dougherty, B., Tomb, J.-F., Fleischmann, R.D.,  
444 Richardson, D., Peterson, J., Kerlavage, A.R., Quackenbush, J., Salzberg, S., Hanson, M., Vugt,  
445 R. van, Palmer, N., Adams, M.D., Gocayne, J., Weidman, J., Utterback, T., Watthey, L.,  
446 McDonald, L., Artiach, P., Bowman, C., Garland, S., Fujii, C., Cotton, M.D., Horst, K., Roberts,  
447 K., Hatch, B., Smith, H.O., Venter, J.C., 1997. Genomic sequence of a Lyme disease spirochaete,  
448 *Borrelia burgdorferi*. *Nature* 390, 580–586. <https://doi.org/10.1038/37551>

449 Goudet, J., 2005. hierfstat, a package for r to compute and test hierarchical F-statistics. *Mol. Ecol.*  
450 Notes 5, 184–186. <https://doi.org/10.1111/j.1471-8286.2004.00828.x>

451 Guttman, D.S., Wang, P.W., Wang, I.N., Bosler, E.M., Luft, B.J., Dykhuizen, D.E., 1996. Multiple  
452 infections of *Ixodes scapularis* ticks by *Borrelia burgdorferi* as revealed by single-strand  
453 conformation polymorphism analysis. *J. Clin. Microbiol.* 34, 652–656.

454 Hanincova, K., Mukherjee, P., Ogden, N.H., Margos, G., Wormser, G.P., Reed, K.D., Meece, J.K.,  
455 Vandermause, M.F., Schwartz, I., 2013. Multilocus Sequence Typing of *Borrelia burgdorferi*  
456 Suggests Existence of Lineages with Differential Pathogenic Properties in Humans. *PLoS ONE*  
457 8, e73066. <https://doi.org/10.1371/journal.pone.0073066>

458 Haven, J., Vargas, L.C., Mongodin, E.F., Xue, V., Hernandez, Y., Pagan, P., Fraser-Liggett, C.M.,  
459 Schutzer, S.E., Luft, B.J., Casjens, S.R., Qiu, W.-G., 2011. Pervasive Recombination and  
460 Sympatric Genome Diversification Driven by Frequency-Dependent Selection in *Borrelia*  
461 *burgdorferi*, the Lyme Disease Bacterium. *Genetics* 189, 951–966.  
462 <https://doi.org/10.1534/genetics.111.130773>

463 Hengge, U.R., Tannapfel, A., Tyring, S.K., Erbel, R., Arendt, G., Ruzicka, T., 2003. Lyme borreliosis.

464 Lancet Infect. Dis. 3, 489–500.  
 465 Kilpatrick, A.M., Dobson, A.D.M., Levi, T., Salkeld, D.J., Swei, A., Ginsberg, H.S., Kjemtrup, A., Padgett,  
 466 K.A., Jensen, P.M., Fish, D., Ogden, N.H., Diuk-Wasser, M.A., 2017. Lyme disease ecology in a  
 467 changing world: consensus, uncertainty and critical gaps for improving control. Philos. Trans. R.  
 468 Soc. Lond. B. Biol. Sci. 372. <https://doi.org/10.1098/rstb.2016.0117>  
 469 Kurtenbach, K., Hanincová, K., Tsao, J.I., Margos, G., Fish, D., Ogden, N.H., 2006. Fundamental  
 470 processes in the evolutionary ecology of Lyme borreliosis. Nat. Rev. Microbiol. 4, 660–669.  
 471 <https://doi.org/10.1038/nrmicro1475>  
 472 Lefterova, M.I., Suarez, C.J., Banaei, N., Pinsky, B.A., 2015. Next-Generation Sequencing for Infectious  
 473 Disease Diagnosis and Management. J. Mol. Diagn. 17, 623–634.  
 474 <https://doi.org/10.1016/j.jmoldx.2015.07.004>  
 475 Li, H., Handsaker, B., Wysoker, A., Fennell, T., Ruan, J., Homer, N., Marth, G., Abecasis, G., Durbin, R.,  
 476 1000 Genome Project Data Processing Subgroup, 2009. The Sequence Alignment/Map format  
 477 and SAMtools. Bioinforma. Oxf. Engl. 25, 2078–2079.  
 478 <https://doi.org/10.1093/bioinformatics/btp352>  
 479 Livey, I., O'Rourke, M., Traweger, A., Savidis-Dacho, H., Crowe, B.A., Barrett, P.N., Yang, X., Dunn, J.J.,  
 480 Luft, B.J., 2011. A new approach to a Lyme disease vaccine. Clin. Infect. Dis. Off. Publ. Infect.  
 481 Dis. Soc. Am. 52 Suppl 3, s266–270. <https://doi.org/10.1093/cid/ciq118>  
 482 Marconi, R.T., Liveris, D., Schwartz, I., 1995. Identification of novel insertion elements, restriction  
 483 fragment length polymorphism patterns, and discontinuous 23S rRNA in Lyme disease  
 484 spirochetes: phylogenetic analyses of rRNA genes and their intergenic spacers in *Borrelia*  
 485 *japonica* sp. nov. and genomic group 21038 (*Borrelia andersonii* sp. nov.) isolates. J. Clin.  
 486 Microbiol. 33, 2427–2434.  
 487 Margos, G., Lane, R.S., Fedorova, N., Koloczek, J., Piesman, J., Hojgaard, A., Sing, A., Fingerle, V.,  
 488 2016. *Borrelia bissettiae* sp. nov. and *Borrelia californiensis* sp. nov. prevail in diverse enzootic  
 489 transmission cycles. Int. J. Syst. Evol. Microbiol. 66, 1447–1452.  
 490 <https://doi.org/10.1099/ijsem.0.000897>  
 491 Margos, G., Marosevic, D., Cutler, S., Derdakova, M., Diuk-Wasser, M., Emler, S., Fish, D., Gray, J.,  
 492 Hunfeldt, K.-P., Jaulhac, B., Kahl, O., Kovalev, S., Kraiczy, P., Lane, R.S., Lienhard, R., Lindgren,  
 493 P.E., Ogden, N., Ornstein, K., Rupprecht, T., Schwartz, I., Sing, A., Straubinger, R.K., Strle, F.,  
 494 Voordouw, M., Rizzoli, A., Stevenson, B., Fingerle, V., 2017. There is inadequate evidence to  
 495 support the division of the genus *Borrelia*. Int. J. Syst. Evol. Microbiol. 67, 1081–1084.  
 496 <https://doi.org/10.1099/ijsem.0.001717>  
 497 Margos, G., Piesman, J., Lane, R.S., Ogden, N.H., Sing, A., Straubinger, R.K., Fingerle, V., 2013. *Borrelia*  
 498 *kurtenbachii* sp. nov.: A widely distributed member of the *Borrelia burgdorferi* sensu lato  
 499 species complex in North America. Int. J. Syst. Evol. Microbiol.  
 500 <https://doi.org/10.1099/ijtsd.0.054593-o>  
 501 Margos, G., Vollmer, S.A., Ogden, N.H., Fish, D., 2011. Population genetics, taxonomy, phylogeny and  
 502 evolution of *Borrelia burgdorferi* sensu lato. Infect. Genet. Evol. 11, 1545–1563.  
 503 <https://doi.org/10.1016/j.meegid.2011.07.022>  
 504 Mechai, S., Margos, G., Feil, E.J., Lindsay, L.R., Ogden, N.H., 2015. Complex population structure of  
 505 *Borrelia burgdorferi* in southeastern and south central Canada as revealed by phylogeographic  
 506 analysis. Appl. Environ. Microbiol. 81, 1309–1318. <https://doi.org/10.1128/AEM.03730-14>  
 507 Mongodin, E.F., Casjens, S.R., Bruno, J.F., Xu, Y., Drabek, E.F., Riley, D.R., Cantarel, B.L., Pagan, P.E.,  
 508 Hernandez, Y.A., Vargas, L.C., Dunn, J.J., Schutzer, S.E., Fraser, C.M., Qiu, W.-G., Luft, B.J.,  
 509 2013. Inter- and intra-specific pan-genomes of *Borrelia burgdorferi* sensu lato: genome stability  
 510 and adaptive radiation. BMC Genomics 14, 693. <https://doi.org/10.1186/1471-2164-14-693>  
 511 Morán Cadenas, F., Rais, O., Humair, P.-F., Douet, V., Moret, J., Gern, L., 2007. Identification of host

512 bloodmeal source and *Borrelia burgdorferi* sensu lato in field-collected *Ixodes ricinus* ticks in  
 513 Chaumont (Switzerland). *J. Med. Entomol.* 44, 1109–1117.

514 Nei, M., 1973. Analysis of gene diversity in subdivided populations. *Proc. Natl. Acad. Sci. U. S. A.* 70,  
 515 3321–3323.

516 Nurk, S., Meleshko, D., Korobeynikov, A., Pevzner, P.A., 2017. metaSPAdes: a new versatile  
 517 metagenomic assembler. *Genome Res.* 27, 824–834. <https://doi.org/10.1101/gr.213959.116>

518 Pritt, Bobbi S., Mead, P.S., Johnson, D.K.H., Neitzel, D.F., Respicio-Kingry, L.B., Davis, J.P., Schiffman,  
 519 E., Sloan, L.M., Schriefer, M.E., Replogle, A.J., Paskewitz, S.M., Ray, J.A., Bjork, J., Steward,  
 520 C.R., Deedon, A., Lee, X., Kingry, L.C., Miller, T.K., Feist, M.A., Theel, E.S., Patel, R., Irish, C.L.,  
 521 Petersen, J.M., 2016. Identification of a novel pathogenic *Borrelia* species causing Lyme  
 522 borreliosis with unusually high spirochaetaemia: a descriptive study. *Lancet Infect. Dis.*  
 523 [https://doi.org/10.1016/S1473-3099\(15\)00464-8](https://doi.org/10.1016/S1473-3099(15)00464-8)

524 Pritt, Bobbi S., Respicio-Kingry, L.B., Sloan, L.M., Schriefer, M.E., Replogle, A.J., Bjork, J., Liu, G.,  
 525 Kingry, L.C., Mead, P.S., Neitzel, D.F., Schiffman, E., Hoang Johnson, D.K., Davis, J.P.,  
 526 Paskewitz, S.M., Boxrud, D., Deedon, A., Lee, X., Miller, T.K., Feist, M.A., Steward, C.R., Theel,  
 527 E.S., Patel, R., Irish, C.L., Petersen, J.M., 2016. *Borrelia mayonii* sp. nov., a member of the  
 528 *Borrelia burgdorferi* sensu lato complex, detected in patients and ticks in the upper midwestern  
 529 United States. *Int. J. Syst. Evol. Microbiol.* 66, 4878–4880.  
 530 <https://doi.org/10.1099/ijsem.0.001445>

531 Qiu, W.-G., 2008. Wide Distribution of a High-Virulence *Borrelia burgdorferi* Clone in Europe and North  
 532 America. *Emerg. Infect. Dis.* 14, 1097–1104. <https://doi.org/10.3201/eid1407.070880>

533 Qiu, W.-G., Dykhuizen, D.E., Acosta, M.S., Luft, B.J., 2002. Geographic Uniformity of the Lyme Disease  
 534 Spirochete (*Borrelia burgdorferi*) and Its Shared History With Tick Vector (*Ixodes scapularis*) in  
 535 the Northeastern United States. *Genetics* 160, 833–849.

536 Qiu, W.-G., Martin, C.L., 2014. Evolutionary genomics of *Borrelia burgdorferi* sensu lato: Findings,  
 537 hypotheses, and the rise of hybrids. *Infect. Genet. Evol.* 27C, 576–593.  
 538 <https://doi.org/10.1016/j.meegid.2014.03.025>

539 Quinlan, A.R., Hall, I.M., 2010. BEDTools: a flexible suite of utilities for comparing genomic features.  
 540 *Bioinforma. Oxf. Engl.* 26, 841–842. <https://doi.org/10.1093/bioinformatics/btq033>

541 R Core Team, 2013. R: A Language and Environment for Statistical Computing. R Foundation for  
 542 Statistical Computing.

543 Rudenko, N., Golovchenko, M., Grubhoffer, L., Oliver, J.H., 2011. *Borrelia carolinensis* sp. nov., a novel  
 544 species of the *Borrelia burgdorferi* sensu lato complex isolated from rodents and a tick from the  
 545 south-eastern USA. *Int. J. Syst. Evol. Microbiol.* 61, 381–383.  
 546 <https://doi.org/10.1099/ijss.0.021436-0>

547 Rudenko, N., Golovchenko, M., Lin, T., Gao, L., Grubhoffer, L., Oliver, J.H., Jr, 2009. Delineation of a  
 548 new species of the *Borrelia burgdorferi* Sensu Lato Complex, *Borrelia americana* sp. nov. *J. Clin.*  
 549 *Microbiol.* 47, 3875–3880. <https://doi.org/10.1128/JCM.01050-09>

550 Schwartz, A.M., Hinckley, A.F., Mead, P.S., Hook, S.A., Kugeler, K.J., 2017. Surveillance for Lyme  
 551 Disease - United States, 2008–2015. *Morb. Mortal. Wkly. Rep. Surveill. Summ. Wash. DC* 2002  
 552 66, 1–12. <https://doi.org/10.15585/mmwr.ss6622a1>

553 Seinost, G., Dykhuizen, D.E., Dattwyler, R.J., Golde, W.T., Dunn, J.J., Wang, I.N., Wormser, G.P.,  
 554 Schriefer, M.E., Luft, B.J., 1999. Four clones of *Borrelia burgdorferi* sensu stricto cause invasive  
 555 infection in humans. *Infect. Immun.* 67, 3518–3524.

556 States, S.L., Brinkerhoff, R.J., Carpi, G., Steeves, T.K., Folsom-O'Keefe, C., DeVeaux, M., Diuk-Wasser,  
 557 M.A., 2014. Lyme disease risk not amplified in a species-poor vertebrate community: similar  
 558 *Borrelia burgdorferi* tick infection prevalence and OspC genotype frequencies. *Infect. Genet.*  
 559 *Evol. J. Mol. Epidemiol. Evol. Genet. Infect. Dis.* 27, 566–575.

560 https://doi.org/10.1016/j.meegid.2014.04.014  
 561 Tilly, K., Casjens, S., Stevenson, B., Bono, J.L., Samuels, D.S., Hogan, D., Rosa, P., 1997. The *Borrelia*  
 562 burgdorferi circular plasmid cp26: conservation of plasmid structure and targeted inactivation  
 563 of the *ospC* gene. *Mol. Microbiol.* 25, 361–373.  
 564 Vidakovic, B., 2011. *Statistics for Bioengineering Sciences: With MATLAB and WinBUGS Support*.  
 565 Springer Science & Business Media.  
 566 Wagemakers, A., Staarink, P.J., Sprong, H., Hovius, J.W.R., 2015. *Borrelia miyamotoi*: a widespread  
 567 tick-borne relapsing fever spirochete. *Trends Parasitol.* 31, 260–269.  
 568 https://doi.org/10.1016/j.pt.2015.03.008  
 569 Walter, K.S., Carpi, G., Evans, B.R., Caccone, A., Diuk-Wasser, M.A., 2016. Vectors as Epidemiological  
 570 Sentinels: Patterns of Within-Tick *Borrelia burgdorferi* Diversity. *PLOS Pathog.* 12, e1005759.  
 571 https://doi.org/10.1371/journal.ppat.1005759  
 572 Wang, G., Liveris, D., Mukherjee, P., Jungnick, S., Margos, G., Schwartz, I., 2014. Molecular Typing of  
 573 *Borrelia burgdorferi*. *Curr. Protoc. Microbiol.* 34, 12C.5.1-31.  
 574 https://doi.org/10.1002/9780471729259.mc12c0534  
 575 Wang, I.-N., Dykhuizen, D.E., Qiu, W., Dunn, J.J., Bosler, E.M., Luft, B.J., 1999. Genetic Diversity of  
 576 *ospC* in a Local Population of *Borrelia burgdorferi* sensu stricto. *Genetics* 151, 15–30.  
 577 Wickham, H., 2009. *Ggplot2: elegant graphics for data analysis*. Springer, Dordrecht; New York.  
 578 Wormser, G.P., Brisson, D., Liveris, D., Hanincová, K., Sandigursky, S., Nowakowski, J., Nadelman, R.B.,  
 579 Ludin, S., Schwartz, I., 2008. *Borrelia burgdorferi* Genotype Predicts the Capacity for  
 580 Hematogenous Dissemination during Early Lyme Disease. *J. Infect. Dis.* 198, 1358–1364.  
 581 https://doi.org/10.1086/592279  
 582

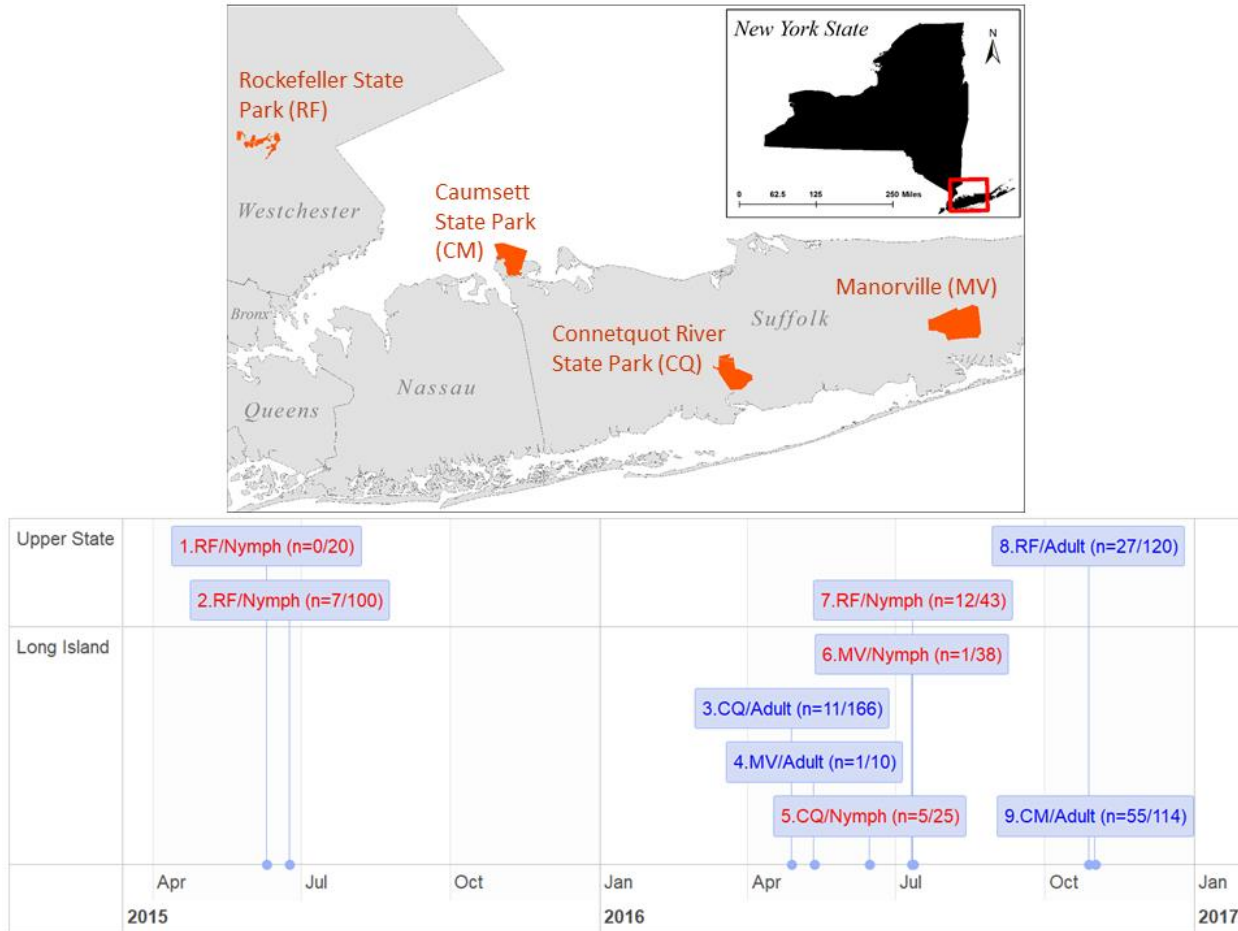
584 **Tables, Figure Legends, & Supporting Information**

585 **Table 1. Allele counts<sup>a</sup>**

A	B	B3	C	C14	D	E	F	G	H	I	J	K	L	M	N	O	T	U	vsp	total
From Upper State, N=27 infected adult ticks (Pop 1)																				
2	4	0	7	0	1	6	0	7	2	3	0	3	4	2	5	0	5	4	2	57
From Upper State, N=19 infected nymphs (Pop 2)																				
3	3	0	1	1	1	4	1	1	3	0	0	2	1	2	2	2	2	0	3	32
From Long Island, N=67 infected adult ticks (Pop 3)																				
12	8	1	4	0	5	12	18	16	10	14	4	17	0	8	8	8	24	13	10	192
From Long Island, N=6 infected nymphs (Pop 4)																				
3	0	0	1	0	0	3	3	2	2	2	3	1	0	3	3	3	0	1	4	34
Sums																				
20	15	1	13	1	7	25	22	26	17	19	7	23	5	15	18	13	31	18	19	315

586 <sup>a</sup>See Figure 5 for allele frequency distributions

587

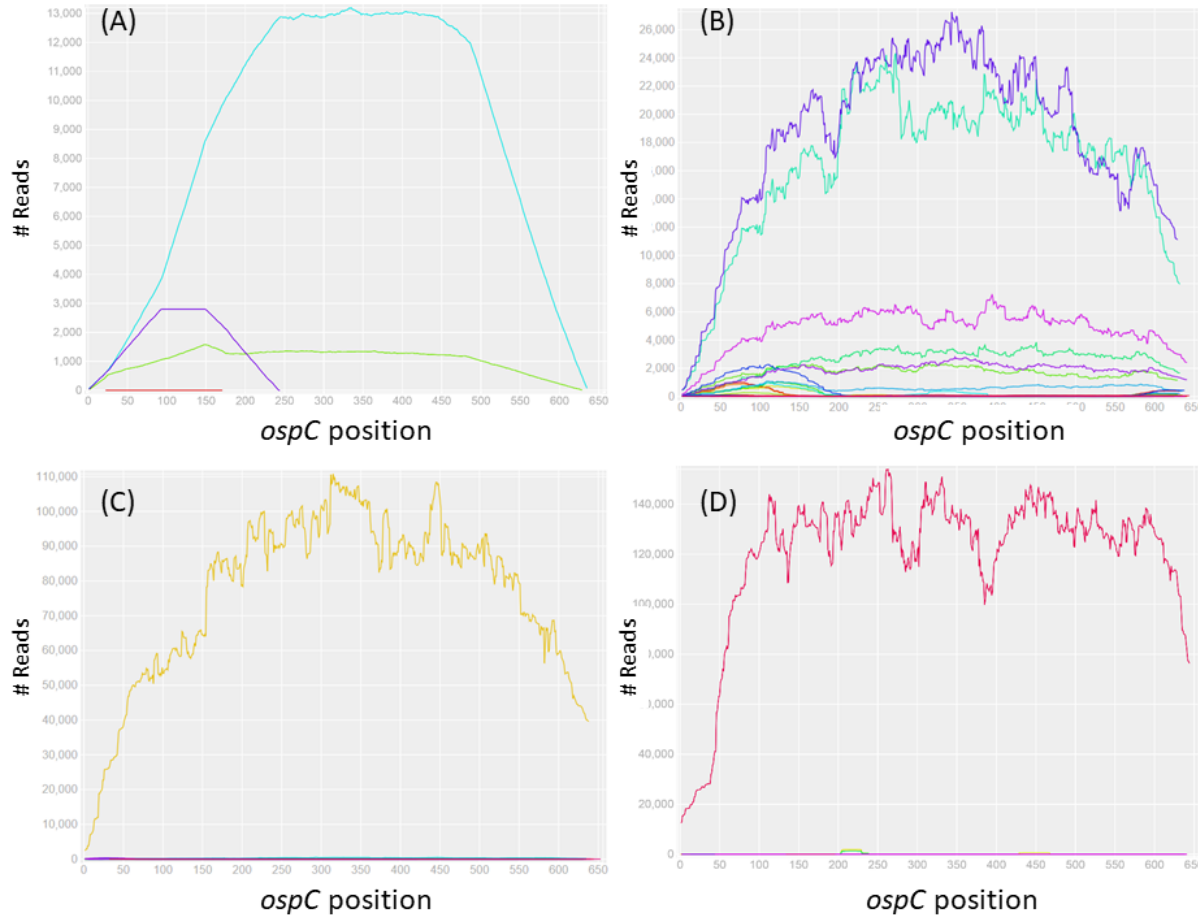


588

589 **Figure 1. Study sites and timeline**

590 Adult and nymphal *Ixodes scapularis* ticks were collected from four study sites in New York State,  
591 US (top) during their host-seeking seasons in a period of 18 months (bottom). Nymphal samples  
592 are colored in red and adult samples in blue. Numbers in parenthesis indicate the number of ticks  
593 infected by Lyme disease spirochetes (numerator) and the total sample size (denominator).

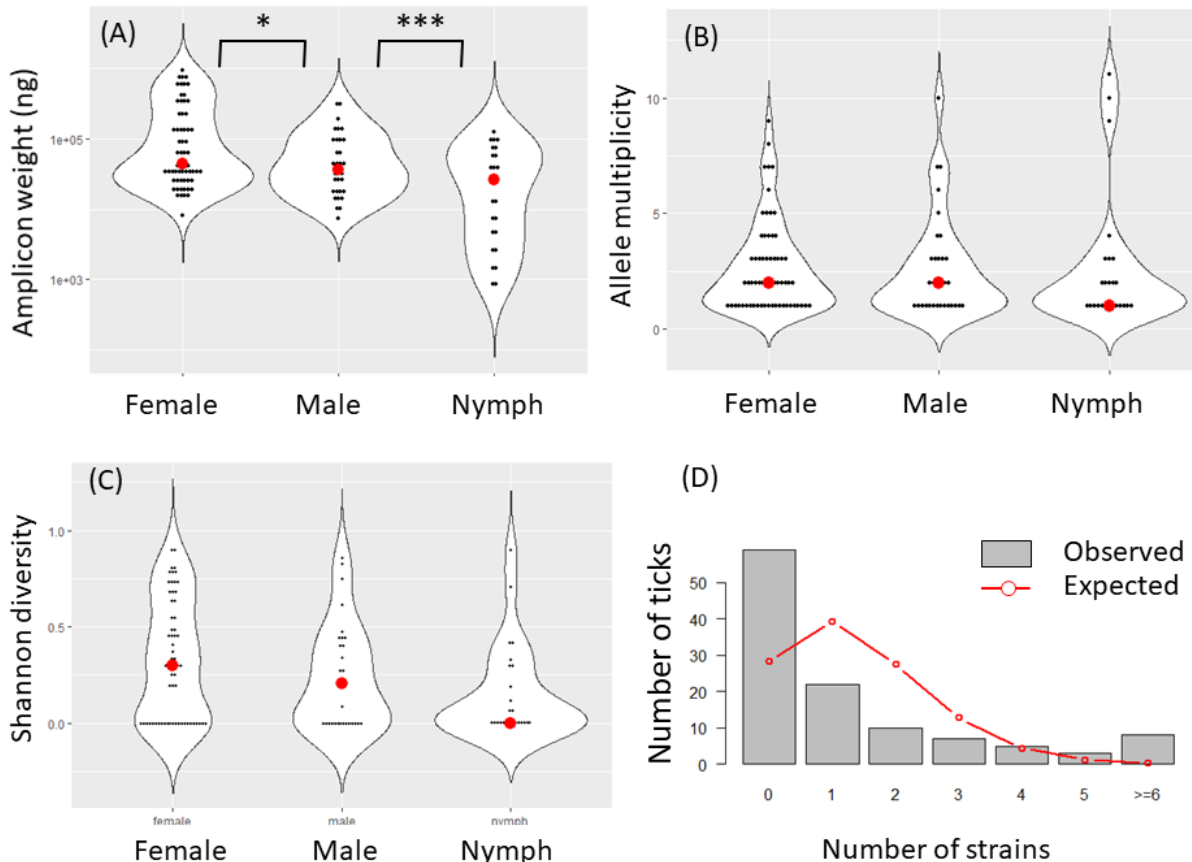
594



595

596 **Figure 2. Read depths of *ospC* alleles in simulated (A) and tick (B, C, D) samples**

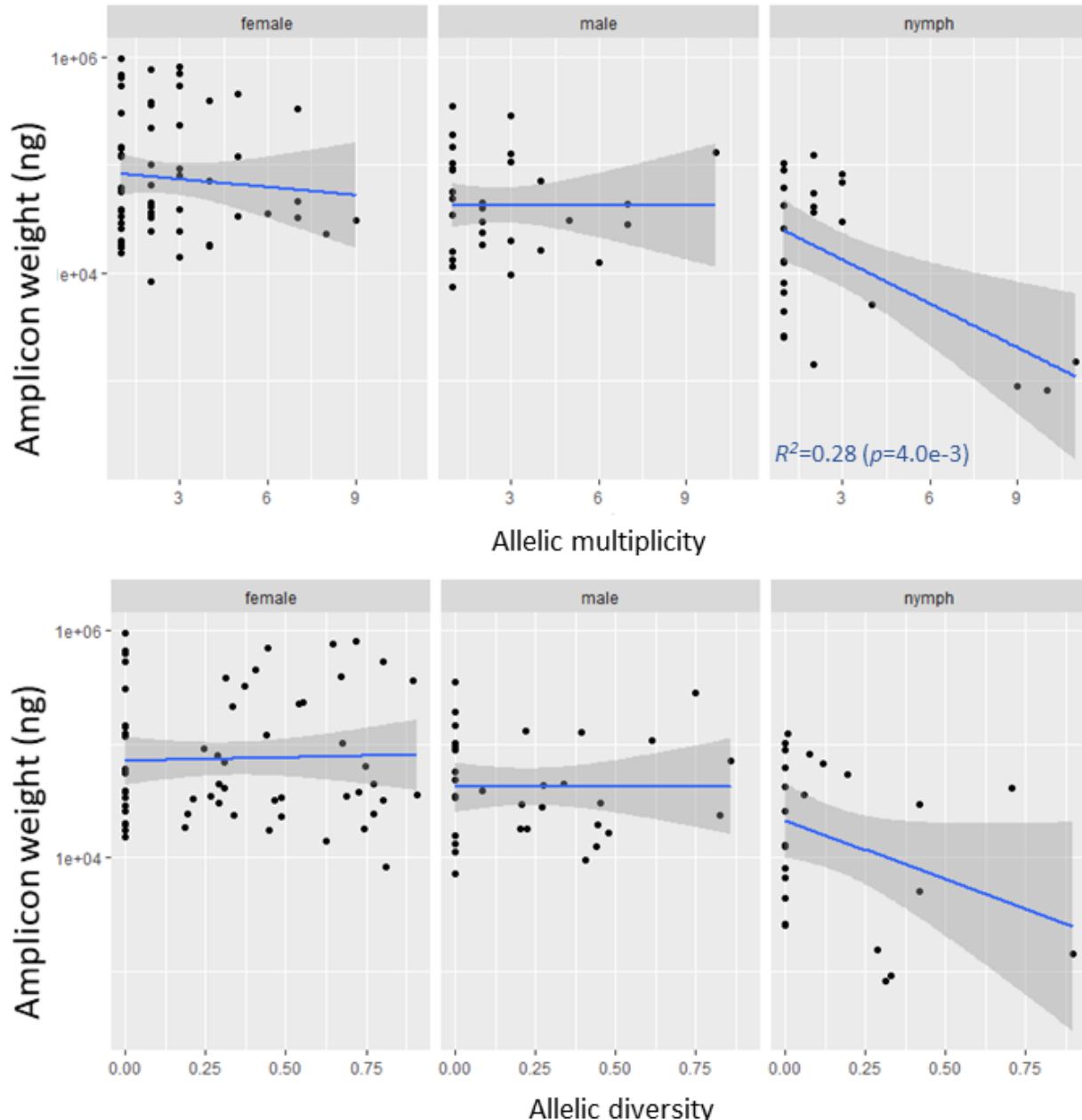
597 (A) Simulated reads are generated based on nucleotide sequences of two *ospC* alleles (J and C)  
598 which are subsequently mixed in a 10:1 proportion. The reads are aligned to all 20 reference  
599 sequences (Supplemental Material S2) and only the two input alleles show complete, full-length  
600 coverages and approximately the same input proportion, validating the specificity and sensitivity  
601 of the bioinformatics protocol for allele identification (a full test of specificity is shown in  
602 Supplemental Material S4). (B) Seven *ospC* alleles (O, I, U, H, T, E, and K) are detected in an  
603 adult tick (#M119, male, RF, Fall 2016). (C) The universal *ospC* primer set is able to amplify not  
604 only the *ospC* locus in *Borrelia* species but also the *vsp* locus in *Borrelia miyamotoi* (see  
605 alignment in Supporting Material S1). Here the *vsp* locus is detected in a nymph tick (#N030, RF,  
606 Summer 2015). (D) A previously unknown *ospC* allele ("C14", GenBank accession MH071431)  
607 is detected in a nymph tick (N150, RF, Summer 2016), suggesting presence of a new *B. bissettiae*-  
608 like species.



609

610 **Figure 3. Spirochete load & diversity**

611 (A) Spirochete loads, estimated with the weight of amplicons (y-axis, log10 scale), are  
612 significantly higher in female ticks than in males ticks, which in turn is higher than in nymphal  
613 ticks. (B) There is no significance differences among the three life stages in strain diversity as  
614 measured by the number of distinct strains within a tick (“multiplicity”). (C) Shannon diversity,  
615 which takes allele frequencies into account (see Material & Methods), is also not significantly  
616 different among the tick stages. These results support the notion that strain diversity in individual  
617 ticks is contributed more by a mixed inoculum in hosts than by the number of blood meals (Walter  
618 et al., 2016). (D) Observed counts of infected and uninfected adult ticks (N=144 from Sample #9,  
619 Figure 1). Expected counts are based on a Poisson model assuming that strains infect ticks  
620 independently. The observed distribution shows an over-abundance of uninfected ticks and ticks  
621 infected by five or more strains, while an under-abundance of ticks infected by 1-3 strains,  
622 suggesting reservoir hosts tend to be either uninfected or repeatedly infected.

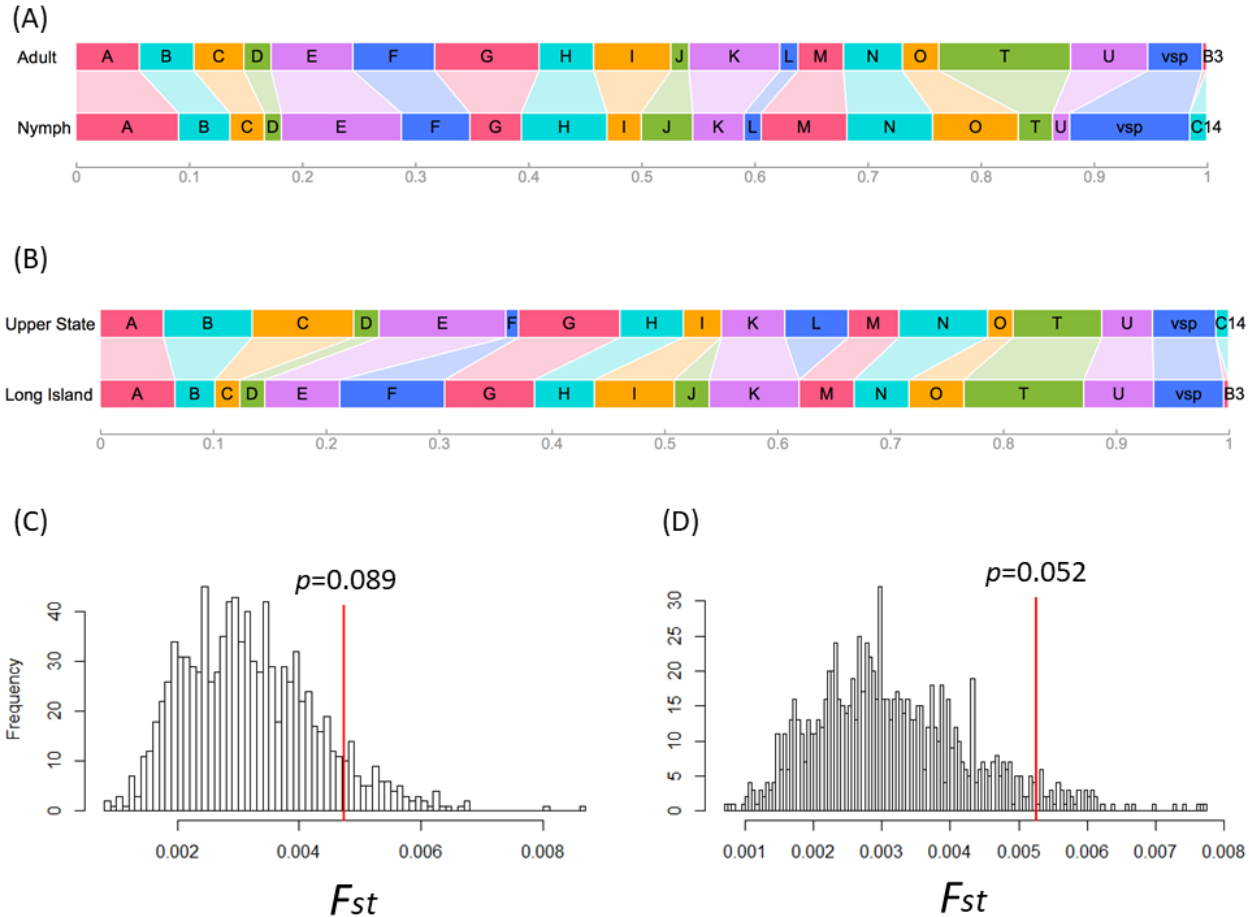


623

624

#### Figure 4. Negative interactions among co-infecting strains

625 (A) Spirochete load is either flat or decreasing with increasing strain multiplicity, supporting  
626 inhibitory interactions among co-infecting strains (Durand et al., 2017; Walter et al., 2016). (B)  
627 The pattern of inhibitory interactions holds when strain diversity is measured by Shannon  
628 diversity.



630 **Figure 5. Geographic and life-stage differences in pathogen strain composition**

631 (A) Strain composition (width of each colored rectangle representing frequency of an allele in a  
 632 population sample) between those infecting adult ticks (Pop1+Pop3, see Table 1) and those  
 633 infecting nymph ticks (Pop2 + Pop4). (B) Strain compositions in two regional populations (Upper  
 634 State, Pop1 + Pop2; Long Island, Pop3 + Pop4;). (C) There is no significant genetic difference in  
 635 strain composition between those infecting adult and those infecting nymph ticks ( $p$  value obtained  
 636 by resampling 999 times; see Material & Methods). (D) Two regional populations show non-  
 637 significant albeit stronger genetic differentiation.

638

639

640 **Supplemental Material**

641 Text S1. Design of universal *ospC* primers for full-length amplification

642 Text S2. Nucleotide sequences of 20 *ospC* alleles used as references for strain identification

643 Text S3. Bioinformatics protocols

644 Figure S4. Specificity of allele identification

645 Figure S5. Strain distribution within infected ticks

646

647